Polymer 69 (2015) 255–263

Contents lists available at ScienceDirect

Polymer

journal homepage: www.elsevier.com/locate/polymer

Recombinant engineering of reversible cross-links into a resilient biopolymer

Elena Degtyar, Barbara Mlynarczyk [1], Peter Fratzl, Matthew J. Harrington*

Department of Biomaterials, Max Planck Institute for Colloids and Interfaces, 14424 Potsdam, Germany

ARTICLE INFO

Article history:
Received 10 December 2014
Received in revised form
9 March 2015
Accepted 10 March 2015
Available online 18 March 2015

Keywords:
Resilin
Self-healing
Histidine-metal coordination

ABSTRACT

Metal coordination bonds are employed in protein based biological materials such as the mussel byssus as reversible sacrificial bonds to achieve autonomic and intrinsic self-healing behavior. In the present study, histidine residues capable of forming coordination bonds were recombinantly engineered into the consensus sequence of resilin, an insect protein that forms a rubbery and resilient biopolymeric network. The purified recombinant resilin mutant, AnG_2His16, was photo cross-linked to form thin films that exhibited a 30-fold increase in modulus compared with wild-type resilin sequences. Addition of Zn^{2+} ions to the mutant resilin films, led to a further increase in stiffness, which, according to Raman spectroscopic studies, arises from His-metal coordination cross-links. These findings show the potential for tuning mechanics and self-healing behavior in biopolymers using bio-engineered metal-binding sites.

1. Introduction

Autonomic and intrinsic self-healing is a defining property of many biological materials, making them an appealing role model for the development of artificial self-healing materials [1]. While the mending of bone and healing of wounds have provided inspiration in the design of self-healing microencapsulated or vascular composites [1–3], metabolically-dependent biological healing processes are incredibly complex at the molecular level, making them somewhat unsuitable as inspiration for the development of self-healing polymers. However, there are also examples of protein-based biological materials that exhibit self-healing properties in the absence of cellular activity. Mechanical properties of proteinaceous biological materials arise as a result of their hierarchical structure – beginning with primary amino acid sequence and secondary structure of the polypeptide chain and ending with multi-scale organization of building blocks and cross-linking strategies [4]. In particular, sacrificial bonding is a biological cross-linking strategy that provides a means of toughening materials, but also provides the potential for material healing if the sacrificial bond is reversible (i.e. can reform once ruptured) [5]. In the context of biological materials, sacrificial bonding refers to non-covalent cross-links embedded in a covalently cross-linked biopolymeric network that rupture before the covalent network; thus, preserving the integrity of the material. In protein-based materials, sacrificial bonds can be hydrogen bonds as in the case of the whelk egg capsule [6], electrostatic bonds as in the case of specific bone associated proteins [7], and as will be discussed in this work, metal coordination bonds as in the case of mussel byssal threads [8].

Metal-coordination bonding is a cross-linking strategy found in a variety of biological materials, which is used to achieve various functionalities due to its combination of high stability and high lability [5]. For example, depending on the intended function of the material, metal fortification is tuned to contribute to hardness, abrasion resistance, adhesive and cohesive properties, as well as to self-healing [5]. Self-healing behavior in such systems is proposed to result from the reversible nature of such bonds. The fact that protein-metal bonds have been shown to exhibit breaking forces half those of covalent bonds [9] makes them even more appealing as reversible cross-links when compared to weaker hydrogen bonds. Metal-dependent self-healing behavior was first proposed in byssal threads of marine mussels [10,11], which serve as attachment fibers for the organism against crashing waves. When byssal threads are stretched beyond their yield point, they are able to dissipate mechanical energy via a large mechanical hysteresis (~70%) during cyclic loading [10]. During subsequent loading cycles, however, the stiffness and energy dissipated are reduced to ~30% of native values. Over time the threads recover their initial properties (i.e. self-heal) [10,12]. This recovery process is proposed to be a

* Corresponding author. Tel.: +49 (0) 331 567 9452.
E-mail address: matt.harrington@mpikg.mpg.de (M.J. Harrington).
[1] Current address: CSM Deutschland GmbH, 55411 Bingen am Rhein.

http://dx.doi.org/10.1016/j.polymer.2015.03.030
0032-3861/

result of restoration of metal-protein bonds coordinated by histidine-rich (His-rich) domains within the primary protein component in the thread [11–14]. Recent studies on peptides based on mussel His-rich protein domains demonstrated the tendency for forming intermolecular His-metal cross-links and highlighted the potential for using such bonds to reinforce biopolymeric networks [15]. Based on these and similar observations on the role of DOPA-metal cross-links in the byssus cuticle [16], synthetic polymers have been produced that incorporate similar metal cross-links, but presently, the extent and range of mechanical behaviors achieved by such systems do not approach those of natural materials [17–20]. This may partly arise from an incomplete understanding of the structure-property relationships that define the biological material (e.g. role of protein sequence, conformation and structural hierarchy).

The aim of the present study is to explore the mechanical influences of the presence of His residues and His-metal coordination bonds in a purely elastic protein-based material. Bioengineering of recombinant biopolymeric proteins provides a convenient platform for this purpose, because protein sequence can be controlled with high precision. Resilin is a rubbery protein found in insect flight and jumping systems that forms a random-network polymer cross-linked chemically through tyrosine (Tyr) residues, generating di- and triTyr linkages [21,22]. Previously, Elvin and co-workers successfully expressed a recombinant resilin construct based on resilin domains from *Anopheles gambiae* and *Drosophila melanogaster* and subsequently produced a bulk material via photo-induced and enzymatic cross-linking of Tyr with mechanical properties comparable to the original resilin proteins [23,24]. Since then, cross-linked recombinant resilin biopolymers with specific consensus sequences from a range of insect species, as well as intentionally modified sequences, have been used to study various questions regarding protein-based materials. In contrast to the energy-dissipating behavior of the byssus, the less stiff resilin-based materials show high resilience over numerous cycles, which arises from an intricate interplay between swelling and cross-link density [25,26]. Thus, based on the proposed role of His-metal bonds in enhancing byssus mechanics, we hypothesize that resilin mechanical behavior can be tuned by recombinant introduction of metal-binding residues into the consensus sequence, resulting in the introduction of strong and reversible cross-links (Fig. 1).

In the present study, consensus sequence from mosquito (*A. gambiae)* resilin protein was selected as the experimental model system. Recombinant resilin-derived proteins were designed to contain 16 identical 11-mer peptide repeats, in which two amino acids per repeat were substituted by His residues. After gene design and construction, a protocol for protein purification and cross-linking was developed, resulting in the production of thin films. Cross-linked films were further analyzed for their mechanical

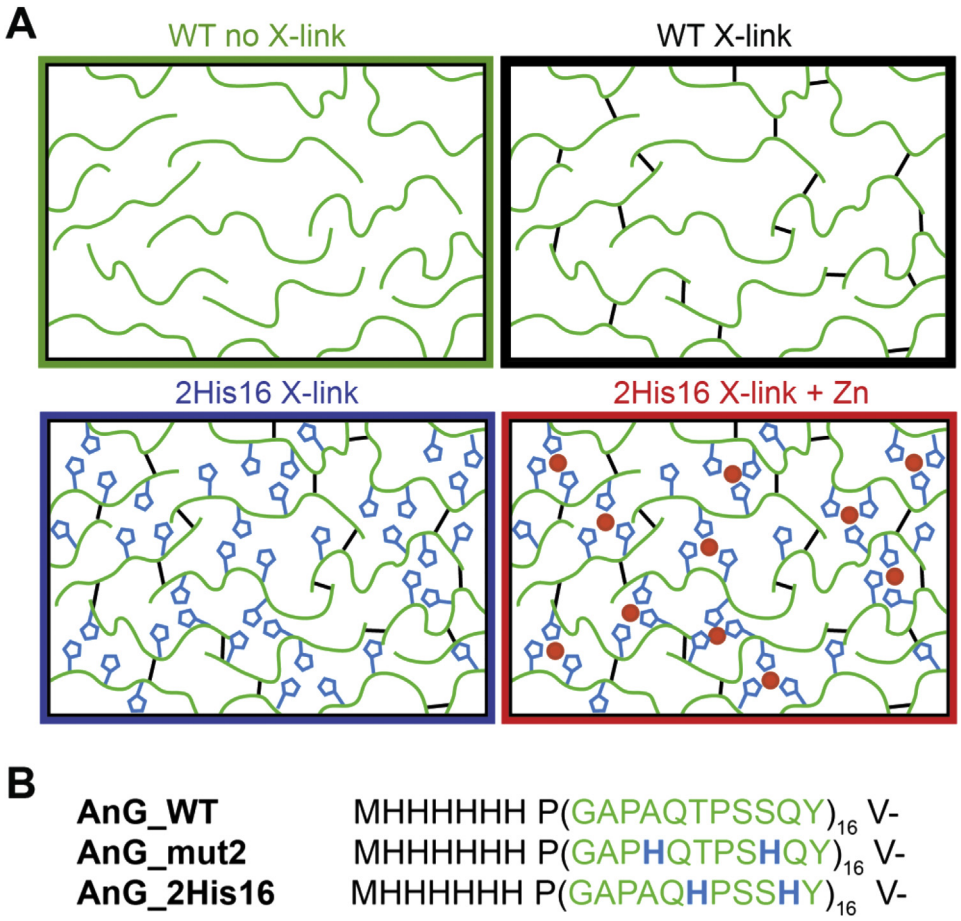

Fig. 1. Schematic of experimental approach. (A) Schematic representation of the rationale behind the experimental design. Wild-type (WT) recombinant resilin protein (green lines) contains no metal-binding residues. Upon photochemical cross-linking of WT X-link, covalent bonds between tyrosine residues (black lines) are formed producing an elastic proteinaceous network. Introduction of histidine residues (blue pentagons) into the sequence allows additional level of cross-linking via metal coordination (red circles). (B) Sequence of the wild type protein (AnG_WT) and two different mutant proteins (AnG_mut2 and AnG_2His16) that were designed.

properties in the presence and absence of metal ions. The current findings demonstrate that by the substitution of only two residues per repeat domain, the stiffness of the material was increased thirty-fold relative to the wild type and was further increased upon addition of Zn^{2+} ions. Raman spectroscopy revealed several possible contributing factors to the increased stiffness, including His-based metal coordination and binuclear metal bridging. These findings highlight the potential for the recombinant production of mechanically tunable and self-healing biopolymers for use in various biomedical and technological applications.

2. Materials and Methods

2.1. Design of 2His16 mutant protein

Wild-type (AnG_WT) and mutated (AnG_2His16) recombinant proteins were based on the resilin consensus sequence from *A. gambiae* (AQTPSSQYGAP). A previously described recursive method for doubling of consensus motifs was used to produce the desired protein constructs [24]. The final proteins (both AnG_WT and AnG_2His16) consist of 16 identical repeats of the eleven-residue consensus sequence. The complimentary oligonucleotides (Sigma–Aldrich, St. Louis, MO) described in Table 1 correspond to one repeat of the consensus sequence, which through annealing created overhang ends of EcoRI (5′ end) and HindIII (3′ end). The oligonucleotides were diluted in annealing buffer (10 mM Tris–HCl buffer, pH 8.0, 1 mM EDTA, 50 mM NaCl) to concentration of 100 μM. 5 μl of each of the oligos was denaturated at 95 °C, then mixed in equimolar concentrations and incubated at 95 °C in water bath for 10 min. The mixtures were then allowed to slowly cool for over 2 h to room temperature. pET22-Nde was digested with EcoRI and HindIII and the annealed primers were ligated into the digested vector. Vectors containing the annealed primers were then transformed into *E. coli* XL1 Blue. These vectors were termed pED-AnG_WT1 and pED-AnG_2His1. Taking advantage of the EcoRI, SmaI and SnaBI restriction sites, the constructs were multiplied to result in 16 consecutive repeats of the consensus sequence (as described in Ref. [24]) to give pED-AnG_WT and pED-AnG_2His16 plasmids. All sequences were verified by sequencing.

2.2. Protein expression

For protein expression, the plasmids were transformed into *E. coli* BL21pLysS expression strain (Invitrogen, Carlsbad, CA). The recombinant proteins were expressed via auto induction method described previously [27]. Bacteria containing appropriate constructs were cultured overnight in 3 ml of LB medium (1% w/v tryptone from casein, 0.5% w/v yeast extract, 1% w/v NaCl) with addition of 100 μg/ml of ampicillin in 37 °C with shaking in 15 ml test tubes. 1.6 ml of the overnight culture was then inoculated into a 2 L Erlenmeyer flask containing 400 ml of ZYP-5052 medium (1% w/v tryptone from casein, 0.5% w/v yeast extract, 25 mM $(NH_4)_2SO_4$, 50 mM KH_2PO_4, 50 mM Na_2HPO_4, 0.5% w/v glycerol, 0.05% w/v glucose, 0.2% w/v α-lactose, 1 mM $MgSO_4$) with addition of 100 μg/ml of ampicillin and 34 μg/ml of chloramphenicol. The protein expression was allowed to proceed for at least 24 h at 37 °C. After incubation, the cells were centrifuged at 6500 g at 4 °C for 20 min. The pellet was stored at −80 °C.

Table 1
Oligonucleotide sequences of primers used for creating pED-AnG_WT1 and pED-AnG_2His1. Codons marked with red in AnG_WT are threonine and glutamine that were exchanged to histidines in AnG_2His.

Oligo	Sequence
AnG_WT Forward	5′ - AATTCCCATACATATGCATCACCATC ACCATCACCCCGGGGCACCGGCGCAAA CCCCGTCTAGCCAGTACGTATAAGGTGATCA
AnG_WT Reverse	5′ - AGCTTGATCACCTTATACGTACTGGCTA GACGGGGTTTGCGCCGGTGCCCCGGGGTG ATGGTGATGGTGATGCATATGTATGGG
AnG_2His Forward	5′ - AATTCCCATACATATGCATCACCATCAC CATCACCCCGGGGCACCGGCGCAACACCCGT CTAGCCACTACGTATAAGGTGATCA
AnG_2His Reverse	5′ - AGCTTGATCACCTTATACGTAGTGGCTA GACGGGTGTTGCGCCGGTGCCCCGGGGTGA TGGTGATGGTGATGCATATGTATGGG

2.3. Protein purification

Purification of AnG_WT was performed according to a previously described protocol [24]. As the final step, the protein was either freeze-dried for 24 h, after which the sample could be stored at room temperature. Alternatively, if the sample was not lyophilized, it could be stored at 4 °C for up to 6 months. For purification of AnG_2His16, a specific protocol was developed. The cell pellet was thawed on ice (pellet from 1 L bacterial culture) and resuspended to homogeneity in 40–60 ml of lysis buffer (250 mM NaCl, 100 mM NaH_2PO_4, 10 mM Tris HCl, pH 7.2, 1% Triton X-100, 1 mM PMSF). Cells were lysed on ice by ultrasonication (6 × 30 s). The cell suspension was then centrifuged at 50,000 g for 1 h at 4 °C. The supernatant was incubated in a 50 °C water bath for 10 min, followed by centrifugation at 12,000 g for 15 min at 20 °C. Urea was added to the supernatant to obtain the final concentration of 8 M. The pH was adjusted to 7.5, and the protein was purified on an NGC Chromatography System (Bio-Rad) using a Ni^{2+}-preloaded 1 ml HiTrap IMAC HP column (GE Healthcare). The column was pre-equilibrated with 10 ml of pre-equilibration buffer (250 mM NaCl, 100 mM NaH_2PO_4, 10 mM Tris HCl, pH 7,2, 1% Triton X-100, 8 M urea, pH 7.5). The crude extract was loaded into the column, and the column was washed with pre-equilibration buffer with increasing concentrations of imidazole as follows: *i.* 6 ml − 40 mM imidazole, *ii.* 8 ml - 100 mM imidazole and *iii.* 7 ml −165 mM imidazole. AnG_2His16 was eluted with 5 ml of elution buffer (250 mM NaCl, 100 mM NaH_2PO_4, 10 mM Tris HCl, 8 M urea, 250 mM imidazole, pH 7.5). The purity of the samples was assessed by SDS-PAGE. The protein fractions were combined and dialyzed overnight against 0.1 M citrate buffer, pH 6.2 followed by 24 h dialysis against double distilled water. Protein composition was verified by amino acid analysis. To this end, proteins were separated on Tris-Tricine gel and transferred to PVDF membrane in the presence of 50 mM CAPS buffer pH 10. The samples were then hydrolyzed for 24 h in the solution containing 6 M HCl with 5% phenol in vacuum at 110 °C. The amino acid composition of the samples was determined using a post-column ninhydrin-based amino acid analyzer (Sykam S433, Fürstenfeldbruck, Germany).

2.4. Photochemical cross-linking and sample preparation

Photochemical cross-linking was performed according to a slightly modified version of a previously published protocol [28,29]. Cross-linking reactions were carried out in a total volume of 20 μl. The final protein concentration was around 1 mg/ml. The final concentration of ruthenium(II) tris-bipyridyl chloride ($Ru(bpy_3)Cl_2$) was 250 μM and the final concentration of ammonium persulfate (APS) was 50 mM. The samples were illuminated for 30 s by a 400 W broad white light lamp with a sample distance of 20 cm from the light source. To follow the progress of cross-linking, aliquots of the cross-linking solution were taken at various time-points and separated on 12% SDS gel. For Raman and AFM measurements, protein cross-linking was performed to form thin films on a glass slide. In

this case, the cross-linking reactions were carried in a total volume of 50 μl. The final protein concentration was around 10–50 mg/ml – dependent on the sample. Afterward, 20 μl of cross-linked sample was transferred to the glass slide and left to dry for 1 h in 37 °C. The samples were washed 3 times with EDTA and then incubated in DDW or PBS pH 7.2. To measure the effect of metal ions on mechanical performance, the dried protein films were extensively washed with 0.1 M Tris–HCl buffer of pH 5.1. The samples were then incubated for at least 12 h with Zn^{2+} ions in the molar ratio of 1:3 of Zn ions to histidine residues. $ZnCl_2$ solution was prepared to the proper concentration in the 0.1 M Tris–HCl buffer of pH 8.1. After the incubation time, extensive washing with 0.1 M Tris–HCl buffer of pH 8.1 was performed to remove unbound metal ions.

2.5. Mechanical testing (AFM)

Mechanical measurements were performed on a Nanowizard III atomic force microsope (AFM) (JPK Instruments AG, Berlin, Germany) in an open cell. The AFM head was mounted on an optical microscope (IX71, Olympus, Japan) with phase contrast optics (objective 63x/1.25 Oil Ph3, Antiflex EC "Plan-Neofluar," Carl Zeiss AG, Germany). To record spatially resolved height and modulus data, the protein films were mapped by an array of AFM force-distance measurements in a 1 μm^2 large grid with 10×10 data points with at least ~150 measurements for each sample. For this purpose we used uncoated silicon cantilevers (CSC 12, Mikromasch, Estonia) with a nominal spring constant of 0.03 N/m. The indentation modulus was calculated from the elastic response of the samples indented by an AFM tip using Hertz model for data fitting [30]. Because the protein network obeys rubber elasticity, a Poisson ratio of 0.5 was assumed. The measurements were performed at constant force of 10 nN. The tip shape was assumed as paraboloid with radius of 20 nm.

2.6. Raman spectroscopy

Raman spectroscopic measurements were performed to assess potential biochemical and structural changes occurring in the various samples. A continuous laser beam was focused down to a micrometer-sized spot on the sample through a confocal Raman microscope (CRM200, WITec, Ulm, Germany) equipped with a piezo-scanner (P-500, Physik Instrumente, Karlsruhe, Germany). The diode-pumped 785 nm near infrared (NIR) laser excitation (Toptica Photonics AG, Graefelfing, Germany) was used in combination with a water immersed 60x (Nikon, NA = 1.0) and a 20x (Nikon, NA = 0.4) microscope objective. The spectra were acquired using a CCD (PI-MAX, Princeton Instruments Inc., Trenton, NJ, USA) behind a grating (300 g mm^{-1}) spectrograph (Acton, Princeton Instruments Inc., Trenton, NJ, USA) with a spectral resolution of approximately 6 cm^{-1}. WiTec Project (v. 2.08, WITec, Ulm, Germany) and OPUS7.0 (Brucker Optic GmbH, Germany) were used for the experimental setup and spectral data processing, respectively.

3. Results and discussion

3.1. Experimental platform design

In the present study, resilin sequence engineering required a rational approach as the goal was to introduce His residues into the sequence without affecting the ability to express the protein or the ability of the expressed protein to cross-link. Analysis of resilin consensus sequences, previously used to produce recombinant proteins for formation of cross-linked hydrogels, revealed no residues capable of coordinating metal ions [24]. In fact, analysis of the evolutionary conserved sequences among at least ten different species showed that His, as well as other charged residues, are rarely present, suggesting that these types of residues would alter the functional integrity of the material [21]. Additionally, this sequence analysis revealed that across different repeats certain residues were more variable than others. Based on this initial survey, two proteins (AnG_2His16 and AnG_mut2) were designed based on the resilin consensus sequence from *A. gambiae* (Fig. 1B), where different residues were substituted for His amino acid in different positions, such that the resulting proteins contain ~20 mol% His – similar to the observed concentration in the mussel proteins [12]. The YGAP (Tyr-Gly-Ala-Pro) sequence was intentionally not altered, because it is highly conserved among all the known resilin proteins, suggesting it has a crucial role in the material's function. The mutant proteins were cloned using previously described recursive method for doubling consensus sequence [24] and recombinantly expressed in *E. coli*. Interestingly, although AnG_mut2 was expressed by the bacteria, it presented a challenge during purification, which may be due slight differences in the hydrophobicity plot of AnG_mut2 construct compared to AnG_WT. Therefore, most of the work was focused on AnG_2His16, whose hydrophobicity characteristics were more similar to the AnG_WT (data not shown).

3.2. Protein purification and photochemical protein cross-linking

The AnG_WT reference protein was successfully purified employing a protocol previously developed by Lyons and colleagues [24] (Fig. 2A). This protocol allows for purification of large amounts of protein permitting sufficiently high concentrations (above 100 mg/ml) required for production of bulk material [23]. As previously reported, the purified protein did not run on the SDS-PAGE gel according to expected AnG_WT molecular weight (MW) (20 kDa), but rather migrated slower through the gel [24]. Unfortunately, the above mentioned purification protocol was found to be unsuitable for purification of the mutant protein AnG_2His16, and an alternative procedure was thus developed. Firstly, PEI precipitation employed in the purification of AnG_WT resulted in precipitation of the mutant and this step was omitted. Secondly, heat resistance analysis showed that, unlike AnG_WT [31], AnG_2His16 was not stable at temperatures above 60 °C (data not shown). Nevertheless, slightly lower temperatures were high enough to remove significant amount of contaminants. Thirdly, co-purified contaminants were present in the final elutions following the Ni-IMAC step. To improve purity, AnG_2His16 was purified under denaturing conditions by adding 8 M urea, which was later removed from the solution by extensive dialysis against citrate buffer at pH 6.2 (Fig. 2B). As with AnG_WT, the mutant migrates on SDS-PAGE above its expected molecular weight (Fig. 2B, arrow head), but in this case, the apparent MW was more than 6-fold larger than the expected MW, strongly suggesting that the mutant can multimerize, even in the presence of SDS. In spite of the slower migration, amino acid analysis performed on the band confirmed the expected protein composition (data not shown). The maximal concentrations of AnG_2His16 obtained using this method did not exceed 10 mg/ml; however, this was still sufficient for efficient cross-linking into thin films.

Protein cross-linking of AnG_WT and AnG_2His16 via diTyr formation was performed using a method originally developed by Fancy and Kodadek [32] and later used by Elvin's group to covalently cross-link not only resilin proteins, but also other proteins that have Tyr residues in their sequence [23,33,34]. Briefly, the method relies on the presence of light harvesting molecule (Ru(II) bpy_3^{2+}) and an electron acceptor (ammonium persulfate) (Fig. 3A) to catalyze formation of covalent diTyr crosslink when exposed to white light (Fig. 3B). DiTyr bonds formed during the process emit blue fluorescent light when illuminated with UV light (ex/em at

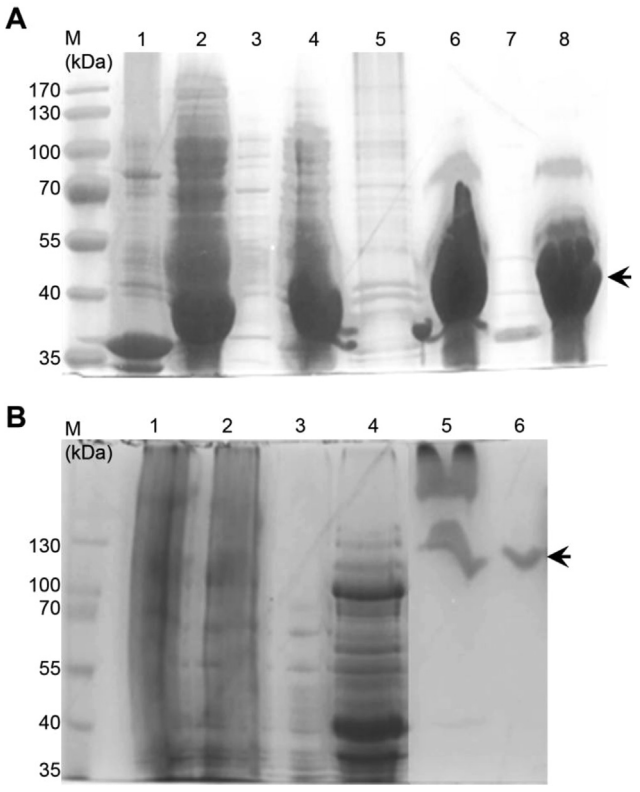

Fig. 2. Protein gels of the purification steps for AnG_WT and AnG_2His16. (A) AnG_WT: lane 1- pellet after sonication; lane 2 - lysate; lane 3 - pellet and lane 4 - lysate following addition of 0.5% of PEI; lane 5 - supernatant and lane 6 - pellet following ammonium sulfate precipitation; lane 7 - pellet and lane 8 - lysate after incubation in 80 °C. The details of the procedure are described in Materials and Methods section. (B) AnG_2His16: lane 1 - pellet and lane 2 - supernatant after sonication; lane 3 - pellet and lane 4 - lysate after incubation at 55 °C; lane 5 - fractions containing the protein; lane 6 - purified AnG_2His16 after dialysis against acetate buffer pH6.2. M indicates the MW marker and arrows depict the protein of interest.

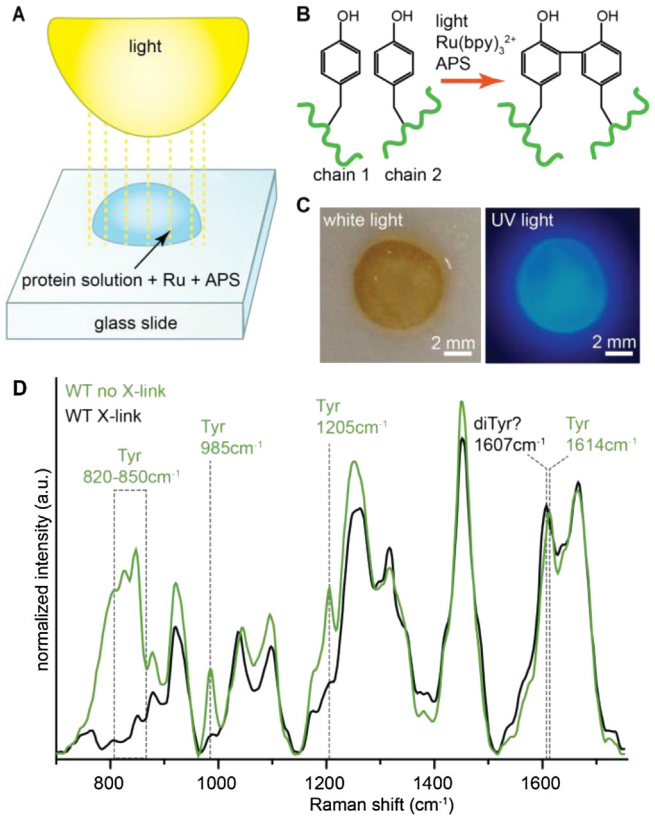

Fig. 3. Photochemical cross-linking of AnG_WT. (A) Illustration of the cross-linking procedure. A drop containing the protein and the cross-linking agents $(Ru(bpy)Cl_3)^{2+}$ and APS was deposited on glass slide and illuminated with white light (300 Watt). (B) Chemical scheme of di-tyrosine bond formation during the illumination. (C) Cross-linked AnG_WT (50 mg/ml) under white light and UV-light. DiTyr bonds emit blue fluorescent light under UV. (D) Raman spectra of AnG_WT protein before (no X-link) and after (X-link) photo cross-linking. Marked are the most pronounced changes observed.

315 nm/409 nm), providing a superficial means of confirming cross-link formation (Fig. 3C). Further analysis of the cross-linked AnG_WT by Raman spectroscopy showed clear changes in several vibrational peaks corresponding to tyrosine (Fig. 3D). The peak at 1614 cm^{-1} observed in the uncross-linked state was previously assigned to Tyr in recombinant resilin [22], and was observed here to shift to 1607 cm^{-1} following photo-induced cross-linking. In addition, a similar shift in the peak at 1044 cm^{-1} was observed, as well as a significant decrease in the intensities of several peaks (985 cm^{-1} and 1205 cm^{-1}), all of which correspond to skeletal vibrations of the tyrosine residues [35]. The most prominent loss of intensity was observed in the characteristic Tyr doublet found in the Raman spectrum at 850 and 830 cm^{-1}. These bands are a result of the Fermi resonance between the benzene ring breathing mode and the overtone of an out-of-plane ring bending vibration of the para-substituted benzenes [36]. The observed changes in the spectrum of the cross-linked AnG_WT clearly indicate a change in the state of Tyr residues in the biopolymer – likely arising from the photo-induced formation of diTyr.

SDS-PAGE gels comparing cross-linking efficiency of AnG_WT and AnG_2His16 are displayed in Fig. 4. The reaction was performed with 2 mg/ml solutions of the respective proteins in an eppendorf tube and was stopped by addition of SDS sample buffer. Efficient cross-linking was completely dependent on the presence of all three cross-linking agents (APS, $Ru(II)_3^{2+}$, light). In both AnG_WT and AnG_2His16, no cross-linking was observed when one of these components was omitted from the experiment. Notably, a distinct higher molecular weight aggregate (above 200 kDa) was observed in the presence of Ru prior to photo-induction in AnG_2His16, but not with AnG_WT, suggesting the possibility of His–Ru bond formation in the mutant. This is not entirely unexpected considering that Ru is known to form highly stable complexes with His residues [37]. The formation of high MW photocross-linking products was dependent on the light exposure time for both proteins. In contrast to AnG_WT, cross-linking products with intermediate MW were not readily observed during AnG_2His16 cross-linking. In fact, even after just 2 s illumination with white light 300 W lamp, the protein was no longer entering the gels, but rather remained almost entirely in the well (Fig. 4B, black arrow head). It is worth mentioning that the samples were boiled prior to application onto the gel, indicating that the aggregates are quite stable and can resist SDS and temperature denaturation.

3.3. Mechanical behavior of cross-linked films

Successful purification and cross-linking of the mutant proteins using the photochemical cross-linking method enabled analysis of the mechanical properties with AFM-based indentation, as previously reported for other recombinant resilin biopolymers [23,38]. Thin films of the respective cross-linked proteins were formed on a glass-surface (Fig. 3A) and were immersed in PBS buffer prior to

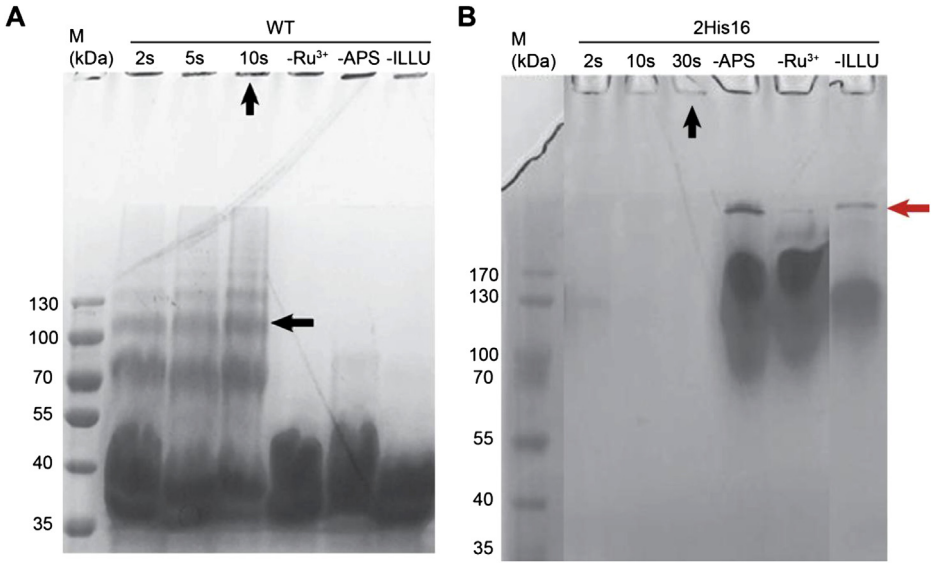

Fig. 4. Protein gels of in vitro cross-linked AnG_WT (A) and AnG_2His16 (B). Each protein solution containing either all of the cross-linking agents or missing one component (-Ru + or − APS or − illumination (illu)) was illuminated for various time lengths and then the resulting products were analyzed on gel. Black arrows indicate high MW protein cross-linking products; red arrow indicates a higher MW product only observed in Ru(II)bpy$_3^{2+}$-containg mixtures without covalent cross-linking. (For interpretation of the references to colour in this figure legend, the reader is referred to the web version of this article.)

mechanical testing, which was performed by applying constant force of 10 nN (Fig. 5A). The extracted indentation moduli values include certain assumptions made concerning the tip-sample interaction [30]; however, considering that all samples were tested in an identical fashion, the relative changes in the indentation moduli provide a valid comparison of stiffness. The measured indentation modulus of AnG_WT was comparable to the previously reported values, averaging ~10 kPa (Fig. 5B) [23,29]. Unexpectedly, the results obtained for AnG_2His16 were almost 30-fold higher at ~285 kPa (Fig. 5C). Given that only 20% of the sequence was altered between AnG_WT and AnG_2His16, this result was verified several times with different protein batches, always with similar results. Possible reasons include His-mediated interactions with Ru, increased efficiency of Tyr-based cross-linking or stiffening of the polymer backbone by His inclusion. Whatever the reason for the observed increase in modulus is, incubation of AnG_2His16 with an excess of Zn^{2+} ions resulted in an additional nearly 3-fold increase in the indentation modulus to ~740 kPa (Fig. 5E). Mechanical tests of AnG_WT in the presence of metal ions showed no observable change in modulus (~10 kPa), despite the presence of His_6-tag on the biopolymer (Fig. 5D). These findings strongly support the proposed hypothesis that the presence of the His residues in the protein sequence can mediate the formation of metal-dependent cross-links that tune mechanical properties.

3.4. Raman spectroscopy of cross-linked films

Raman spectra of cross-linked AnG_WT and AnG_2His16 appear to be similar, suggesting that the resilin biopolymer is not perturbed excessively by the introduction of His residues (Fig. 6A). Importantly, Tyr-related peaks are very similar between AnG_WT and AnG_2His16, indicating that diTyr cross-linking was also successful for the mutant. Nonetheless, there are some obvious distinctions between the spectra that are further highlighted and

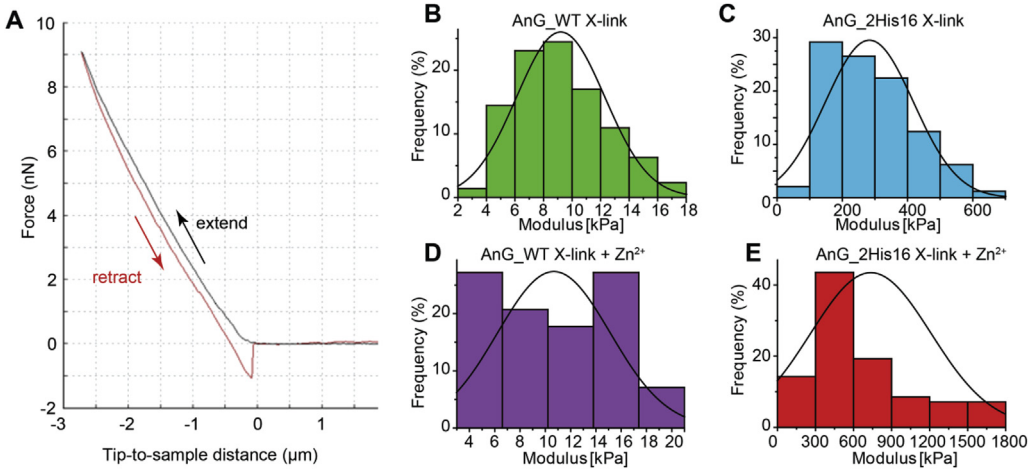

Fig. 5. AFM-based mechanical testing of cross-linked AnG_WT and AnG_2His16 with and without Zn^{2+}. A) Typical force-displacement curve for hydrated AnG_WT. B-E) Histograms of indentation moduli for AnG_WT and AnG_2His16 with and without Zn^{2+} ions present. The mean value for AnG_WT (B) was ~9 kPa, while for AnG_2His16 (C) was ~285 kPa. Upon addition of Zn^{2+}, the mean value for AnG_WT (D) remained constant at ~10 kPa, while for AnG_2His16 (E) the mean was increased to ~740 kPa.

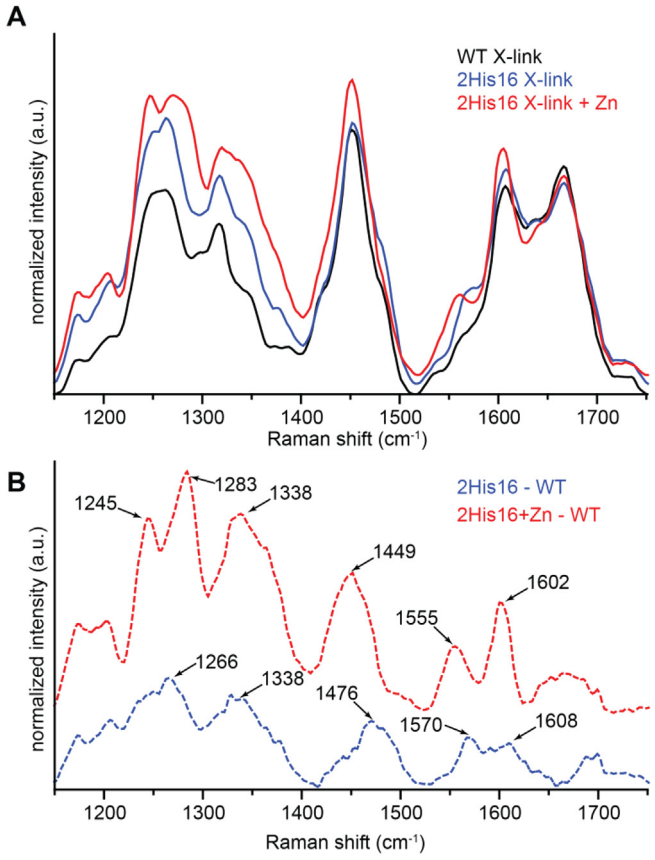

Fig. 6. Raman spectra of cross-linked WT and 2His16 resilin. A) Spectra of AnG_WT resilin compared with AnG_2His16 with and without Zn added. B) Difference spectra of AnG_2His16 Raman spectra with and without Zn as compared to the AnG_WT spectrum. Prominent peaks are indicated.

accentuated in the difference spectra (Fig. 6B), The most notable differences between the spectra of cross-linked AnG_WT and AnG_2His16 are peaks centered at 1570 cm^{-1} and 1266 cm^{-1}, both of which are consistent with the presence of deprotonated His (Takeuchi 2003). Upon addition of Zn^{2+} to the cross-linked AnG_2His16 (Fig. 6A and B), the appearance of a sharp peak in the difference spectrum at 1602 cm^{-1} indicates the presence of metal coordinated His [39]. Additionally, a clear peak at 1560 cm^{-1} and a shoulder at ~1283 cm^{-1} in the Raman spectrum of AnG_2His16 + Zn^{2+} indicate the presence of bridging His imidazolate side chains, which are bound to two metal ions per residue [39]. The similarity of the amide I band in all three spectra indicates that there is no significant change in secondary structure by the addition of His residues regardless of whether metal ions are present or not (i.e. the structure remains essentially disordered) [22].

The results of this study provide compelling evidence that bioengineering of His residues into the soft elastic protein network of recombinant resilin can alter the mechanical performance, resulting in an overall nearly 80-fold increase in stiffness in the presence of metal ions. Raman spectroscopy suggests that this occurs at least partially due to His-mediated protein-metal cross-links with both mononuclear and binuclear coordination states (Fig. 6). However, the 30-fold increase in modulus observed between AnG_WT and AnG_2His16 cross-linked films before adding Zn^{2+} ions was unexpected and deserves comment. In light of the current results, three mechanisms seem plausible – 1. The mere presence of His residues induces stiffening of the biopolymer network; 2. The presence of His residues influences the diTyr cross-linking efficiency during photo-polymerization; 3. Ru-His intermolecular cross-links remain in the material after photochemical cross-linking, contributing to mechanics. It is important to note that these possibilities are not mutually exclusive and may all contribute. Each potential mechanism is discussed individually below.

The first possibility is that the unexpected increase in stiffness is simply a result of the introduction of His residues into the resilin sequence. In examining the variety of known resilin sequences from different organisms, His residues are almost entirely excluded, whereas almost all other residues, besides Cys, are represented to some degree [21]. This may suggest that including His in the consensus sequence has been avoided evolutionarily, perhaps for the very reason that it alters the material properties even at low composition. In nature, there are examples of His-rich biological materials, including the sucker rings of jumbo squids (*Dosidicus gigas)* that exhibit stiff mechanical behavior (E = 6–8 GPa) in the absence of metal ions or any covalent cross-links [40]. While the exact contribution of His in this material is unknown, the His-rich proteins comprising the sucker rings were found to form silk-like arrangements of beta-crystallites stabilized in the absence of a covalent cross-linking network. Likewise, the high modulus (~3 GPa) of *Nereis* worm jaws following metal ion depletion by EDTA treatment [41] was also attributed to specific protein structure and hierarchical organization of the His-rich protein building blocks [42]. In these two systems, it has not been possible to differentiate the contribution of His vis-á-vis secondary structure to the observed mechanical behavior in the absence of metal ions. In the present study, Raman spectra of AnG_2His16 do not indicate the presence of any well-defined secondary structure (e.g. β-sheet and α-helix); however, it is conceivable that a simple change in sequence might result in the observed increase in stiffness of the polymer chains.

It is also plausible that the presence of His residues in AnG_2His16 increases the efficiency of diTyr formation during the photopolymerization process, resulting in an increase of stiffness. Previously, it was reported that 20% of all Tyr residues present in the YGAP conserved sequence would form di-Tyr bonds, while in the natural material it can be as high as 25% [23]. Increased cross-linking efficiency could occur if the biopolymers were initially linked via His-Ru metal coordination (as suggested by the high MW band in Fig. 4B) bringing more Tyr residues into proximity during the photochemical reaction. This effect was previously demonstrated to be an effective means of increasing cross-link efficiency in His-containing model peptides [43]. The Raman spectroscopy of cross-linked AnG_WT and AnG_2His16, however, appear similar in regards to the intensity of the Tyr peaks suggesting that the cross-linking efficiency may be similar.

Another possible mechanism for the observed stiffening of AnG_2His16 vis-à-vis AnG_WT is the formation of intermolecular His-Ru^{2+} metal coordination bonds. As already mentioned, this hypothesis is supported by the observation of a distinct higher MW multimer (>200 kDa) in SDS-PAGE gels in the reaction mixtures with Ru prior to photo-polymerization, but not in the absence of Ru (Fig. 4B). While the biopolymeric films were washed extensively with EDTA prior to mechanical testing in order to deplete them of any residual metals, His-Ru complexes are known to be exceptionally stable [37,44] and possibly resistant to this treatment. The presence of Raman peaks indicating binuclear metal binding sites bridged by a single His residue upon addition of Zn^{2+} ions offers further support for the presence of His-Ru bonds in AnG_2His16 films (Fig. 6). Due to the very high pKa of the pyrrole hydrogen of the His imidazole side group (~14.2), binuclear metal sites bridged by His are only rarely observed in nature such as in the case of superoxide dismutase and αβ amyloid fibers [45,46]. Under

physiological conditions this proton should not ionize; however, this is possible if local conditions lead to a lowering of the pK_a. Notably, previous studies on imidazole (the side chain of His) have demonstrated a reduction of the pK_a of the imidazole pyrrole hydrogen by more than 5 units from 14.2 to 8.9 when the imidazole group is bound to Ru [47], bringing it within a range relevant to the current study. It is, therefore, highly plausible that the Ru used in the photopolymerization process remains bound to His following cross-linking, and that when an excess of Zn is added, the pyrrole hydrogen of the imidazole side group is removed, leading to additional coordination of Zn by His residues. Creation of metal coordination bridges effectively increases the number of cross-links in the network, possibly providing the further 3-fold increase of the stiffness. If confirmed, the use of Ru to lower the pKa could provide a novel mechanism for tuning mechanical behavior of His-based metallopolymers.

All three mechanisms discussed could potentially contribute to the 30-fold increase in modulus observed before Zn is added. However, based on the evidence of Ru interaction with His residues during and after cross-linking, the latter two mechanisms seem most probable. One possible means of determining if the increased stiffness in 2His16 is Ru-dependent would be to perform cross-linking of films by another means that does not include metal ions. For example, previous studies have demonstrated that it is also possible to cross-link recombinant resilin (and other Tyr containing proteins) with the enzyme tyrosinase [48]. While it was possible to cross-link recombinant resilin with tyrosinase, photopolymerization with Ru was found to yield more consistent results, making it the preferred method in the field [23]. Future work will focus on optimizing protein yield and alternative cross-linking strategies in order to further explore the effect of single amino acid substitutions on mechanical properties of recombinant resilin.

4. Conclusions

Regardless of the exact mechanisms leading to the observed mechanical properties of the His-rich biopolymer, these results demonstrate the strong potential for bio-engineering load-bearing metal-binding sites into biopolymers for the purpose of altering material performance. The His residues engineered into the resilin consensus sequence in the present study were shown to increase mechanical stiffness by up to 80-fold, which is at least partially due to the introduction of His-metal cross-links. While the present study highlights the potential for increasing modulus via His-introduction, future studies will focus on investigating their possible mechanical contribution to viscoelastic properties and self-healing behavior. For example, if these load-bearing bonds are ruptured during stretching, then there is strong reason to believe that they will reform upon recoil of the elastic resilin network – possibly leading to mechanical recovery. The potential for His-metal cross links to function as mechanically reversible bonds is supported by previous works on synthetic polymers in which hydrogels have been created with sacrificial metal-coordination bonds embedded in a covalent network [17,49]. As opposed to synthetic polymers, however, biopolymer properties and their derived materials depend not only on cross-link type and density, but also on the sequence of the protein or peptide used – providing the possibility for precise alteration of functional groups, which can have large effects across multiple length scales.

Acknowledgments

The authors thank the German Research Foundation (DFG, Individual Research Grant HA6369/3-1) and the Max Planck Society for financial support. We thank Y. Politi for helpful discussion and J. Steffen for technical assistance.

References

[1] Chen P-Y, McKittrick J, Meyers MA. Biological materials: functional adaptations and bioinspired designs. Prog Mater Sci 2012;57(8):1492–704. http://dx.doi.org/10.1016/j.pmatsci.2012.03.001.
[2] Kessler M, Sottos N, White S. Self-healing structural composite materials. Compos Part A Appl Sci Manuf 2003;34(8):743–53. http://dx.doi.org/10.1016/S1359-835X(03)00138-6.
[3] Toohey KS, Sottos NR, Lewis JA, Moore JS, White SR. Self-healing materials with microvascular networks. Nat Mater 2007;6(8):581–5. http://dx.doi.org/10.1038/nmat1934.
[4] Buehler MJ. Tu(r)ning weakness to strength. Nano Today 2010;5(5):379–83. http://dx.doi.org/10.1016/j.nantod.2010.08.001.
[5] Degtyar E, Harrington MJ, Politi Y, Fratzl P. The mechanical role of metal ions in biogenic protein-based materials. Angew Chem Int Ed 2014;53(45):12026–44. http://dx.doi.org/10.1002/anie.201404272. n/a–n/a.
[6] Miserez A, Wasko SS, Carpenter CF, Waite JH. Non-entropic and reversible long-range deformation of an encapsulating bioelastomer. Nat Mater 2009;8(11):910–6. http://dx.doi.org/10.1038/nmat2547.
[7] Fantner GE, Hassenkam T, Kindt JH, Weaver JC, Birkendal H, Pechenik L, et al. Sacrificial bonds and hidden length dissipate energy as mineralized fibrils separate during bone fracture. Nat Mater 2005;4(8):612–6. http://dx.doi.org/10.1038/nmat1428.
[8] Harrington MJ, Waite JH. How nature modulates a fiber's mechanical properties: mechanically distinct fibers drawn from natural mesogenic block copolymer variants. Adv Mater 2009;21(4):440–4. http://dx.doi.org/10.1002/adma.200801072.
[9] Lee H, Scherer NF, Messersmith PB. Single-molecule mechanics of mussel adhesion. Proc Natl Acad Sci U S A 2006;103(35):12999–3003. http://dx.doi.org/10.1073/pnas.0605552103.
[10] Carrington E, Gosline J. Mechanical design of mussel byssus: load cycle and strain rate dependence. Am Malacol Bull 2004;18:135–42. Available at: http://faculty.washington.edu/ecarring/AmMalBul.pdf [accessed 12.06.13].
[11] Vaccaro E, Waite JH. Yield and post-yield behavior of mussel byssal thread: a self-healing biomolecular material. Biomacromolecules 2001;2(3):906–11. Available at: http://www.ncbi.nlm.nih.gov/pubmed/11710048.
[12] Harrington MJ, Waite JH. Holdfast heroics: comparing the molecular and mechanical properties of Mytilus californianus byssal threads. J Exp Biol 2007;210(24):4307–18. http://dx.doi.org/10.1242/Jeb.009753.
[13] Krauss S, Metzger TH, Fratzl P, Harrington MJ. Self-repair of a biological fiber guided by an ordered elastic framework. Biomacromolecules 2013;14(5):1520–8. http://dx.doi.org/10.1021/bm4001712.
[14] Harrington MJ, Gupta HS, Fratzl P, Waite JH. Collagen insulated from tensile damage by domains that unfold reversibly: in situ X-ray investigation of mechanical yield and damage repair in the mussel byssus. J Struct Biol 2009;167(1):47–54. http://dx.doi.org/10.1016/j.jsb.2009.03.001.
[15] Schmidt S, Reinecke A, Wojcik F, Pussak D, Hartmann L, Harrington MJ. Metal-mediated molecular self-healing in histidine-rich mussel peptides. Biomacromolecules 2014;15(5):1644–52. http://dx.doi.org/10.1021/bm500017u.
[16] Harrington MJ, Masic A, Holten-Andersen N, Waite JH, Fratzl P. Iron-clad fibers: a metal-based biological strategy for hard flexible coatings. Science 2010;328(5975):216–20. http://dx.doi.org/10.1126/science.1181044 (80-).
[17] Barrett DG, Fullenkamp DE, He L, Holten-Andersen N, Lee KYC, Messersmith PB. Ph-based Regulation of hydrogel mechanical properties through mussel-inspired Chemistry and processing. Adv Funct Mater 2013;23(9):1111–9. http://dx.doi.org/10.1002/adfm.201201922.
[18] Holten-Andersen N, Harrington MJ, Birkedal H, Lee BP, Messersmith PB, Lee KYC, et al. pH-induced metal-ligand cross-links inspired by mussel yield self-healing polymer networks with near-covalent elastic moduli. Proc Natl Acad Sci U S A 2011;108(7):2651–5. http://dx.doi.org/10.1073/pnas.1015862108.
[19] Holten-Andersen N, Jaishankar A, Harrington MJ, Fullenkamp DE, DiMarco G, He L, et al. Metal-coordination: using one of nature's tricks to control soft material mechanics. J Mater Chem B 2014;2(17):2467. http://dx.doi.org/10.1039/c3tb21374a.
[20] Fullenkamp DE, He L, Barrett DG, Burghardt WR, Messersmith PB. Mussel-inspired histidine-based transient network metal coordination hydrogels. Macromolecules 2013;46(3):1167–74. http://dx.doi.org/10.1021/ma301791n.
[21] Andersen SO. Studies on resilin-like gene products in insects. Insect Biochem Mol Biol 2010;40(7):541–51. http://dx.doi.org/10.1016/j.ibmb.2010.05.002.
[22] Nairn KM, Lyons RE, Mulder RJ, Mudie SR, Cookson DJ, Lesieur E, et al. A synthetic resilin is largely unstructured. Biophys J 2008;95(7):3358–65. http://dx.doi.org/10.1529/biophysj.107.119107.
[23] Elvin CM, Carr AG, Huson MG, Maxwell JM, Pearson RD, Vuocolo T, et al. Synthesis and properties of crosslinked recombinant pro-resilin. Nature 2005;437(7061):999–1002. http://dx.doi.org/10.1038/nature04085.
[24] Lyons RE, Lesieur E, Kim M, Wong DCC, Huson MG, Nairn KM, et al. Design and facile production of recombinant resilin-like polypeptides: gene construction and a rapid protein purification method. Protein Eng Des Sel 2007;20(1):25–32. http://dx.doi.org/10.1093/protein/gzl050.

[25] Truong MY, Dutta NK, Choudhury NR, Kim M, Elvin CM, Nairn KM, et al. The effect of hydration on molecular chain mobility and the viscoelastic behavior of resilin-mimetic protein-based hydrogels. Biomaterials 2011;32(33):8462–73. http://dx.doi.org/10.1016/j.biomaterials.2011.07.064.
[26] Kim M, Tang S, Olsen BD. Physics of engineered protein hydrogels. J Polym Sci Part B Polym Phys 2013;51(7):587–601. http://dx.doi.org/10.1002/polb.23270.
[27] Studier FW. Protein production by auto-induction in high density shaking cultures. Protein Expr Purif 2005;41(1):207–34. Available at: http://www.ncbi.nlm.nih.gov/pubmed/15915565.
[28] Fancy DA, Denison C, Kim K, Xie Y, Holdeman T, Amini F, et al. Scope, limitations and mechanistic aspects of the photo-induced cross-linking of proteins by water-soluble metal complexes. Chem Biol 2000;7(9):697–708. Available at: http://www.ncbi.nlm.nih.gov/pubmed/10980450.
[29] Lyons RE, Nairn KM, Huson MG, Kim M, Dumsday G, Elvin CM. Comparisons of recombinant resilin-like proteins: repetitive domains are sufficient to confer resilin-like properties. Biomacromolecules 2009;10(11):3009–14. http://dx.doi.org/10.1021/bm900601h.
[30] Maxwell JM, Huson MG. Scanning probe microscopy examination of the surface properties of keratin fibres. Micron 2005;36(2):127–36. http://dx.doi.org/10.1016/j.micron.2004.10.001.
[31] Kim M, Elvin C, Brownlee A, Lyons R. High yield expression of recombinant pro-resilin: lactose-induced fermentation in E. coli and facile purification. Protein Expr Purif 2007;52(1):230–6. http://dx.doi.org/10.1016/j.pep.2006.11.003.
[32] Fancy D a, Kodadek T. Chemistry for the analysis of protein-protein interactions: rapid and efficient cross-linking triggered by long wavelength light. Proc Natl Acad Sci U S A 1999;96(11):6020–4. Available at: http://www.pubmedcentral.nih.gov/articlerender.fcgi?artid=26828&tool=pmcentrez&rendertype=abstract.
[33] Elvin CM, Vuocolo T, Brownlee AG, Sando L, Huson MG, Liyou NE, et al. A highly elastic tissue sealant based on photopolymerised gelatin. Biomaterials 2010;31(32):8323–31. http://dx.doi.org/10.1016/j.biomaterials.2010.07.032.
[34] Elvin CM, Brownlee AG, Huson MG, Tebb TA, Kim M, Lyons RE, et al. The development of photochemically crosslinked native fibrinogen as a rapidly formed and mechanically strong surgical tissue sealant. Biomaterials 2009;30(11):2059–65. http://dx.doi.org/10.1016/j.biomaterials.2008.12.059.
[35] Tsuboi M, Ezaki Y, Aida M, Suzuki M, Yimit A, Ushizawa K, et al. Raman scattering tensors of tyrosine. Biospectroscopy 1998;4(1):61–71. 10.1002/(SICI)1520-6343(1998)4:13.0.CO;2-V.
[36] Siamwiza M, Lord R, Chen M. Interpretation of the doublet at 850 and 830 cm-1 in the Raman spectra of tyrosyl residues in proteins and certain model compounds. Biochemistry 1975;14(22):4870–6. Available at: http://pubs.acs.org/doi/abs/10.1021/bi00693a014 [accessed 6.11.14].
[37] Arnold FH, Zhang JH. Metal-mediated protein stabilization. Trends Biotechnol 1994;12(5):189–92. http://dx.doi.org/10.1016/0167-7799(94)90081-7.
[38] Qin G, Rivkin A, Lapidot S, Hu X, Preis I, Arinus SB, et al. Recombinant exon-encoded resilins for elastomeric biomaterials. Biomaterials 2011;32(35):9231–43. Available at: http://dx.doi.org/10.1016/j.biomaterials.2011.06.010 [accessed 30.07.12].
[39] Takeuchi H. Raman structural markers of tryptophan and histidine side chains in proteins. Biopolymers 2003;72(5):305–17. http://dx.doi.org/10.1002/bip.10440.
[40] Guerette PA, Hoon S, Seow Y, Raida M, Masic A, Wong FT, et al. Accelerating the design of biomimetic materials by integrating RNA-seq with proteomics and materials science. Nat Biotechnol 2013;31(10):908–15. http://dx.doi.org/10.1038/nbt.2671.
[41] Broomell CC, Mattoni MA, Zok FW, Waite JH. Critical role of zinc in hardening of Nereis jaws. J Exp Biol 2006;209(Pt 16):3219–25. http://dx.doi.org/10.1242/jeb.02373.
[42] Broomell CC, Chase SF, Laue T, Waite JH. Cutting edge structural protein from the jaws of Nereis virens. Biomacromolecules 2008;9(6):1669–77. http://dx.doi.org/10.1021/bm800200a.
[43] Stayner RS, Min D-J, Kiser PF, Stewart RJ. Site-specific cross-linking of proteins through tyrosine hexahistidine tags. Bioconjug Chem 2005;16(6):1617–23. http://dx.doi.org/10.1021/bc050249b.
[44] Umaña P, K Jr J, Arnold F. Recombinant protein stabilization through engineered metal-chelating sites. 1993. p. 102–8. Available at: http://www.lw20.com/2011061069330671.html [accessed 17.10.14].
[45] Curtain CC, Ali F, Volitakis I, Cherny RA, Norton RS, Beyreuther K, et al. Alzheimer's disease amyloid-beta binds copper and zinc to generate an allosterically ordered membrane-penetrating structure containing superoxide dismutase-like subunits. J Biol Chem 2001;276(23):20466–73. http://dx.doi.org/10.1074/jbc.M100175200.
[46] Strothkamp KG, Lippard SJ. Chemistry of the imidazolate-bridged bimetallic center in the copper-zinc superoxide dismutase and its model compounds. Acc Chem Res 1982;15(10):318–26. http://dx.doi.org/10.1021/ar00082a004.
[47] Hoq MF, Shepherd RE. Influence of the metal centers on the pKa of the pyrrole hydrogen of imidazole complexes of (NH3)53+, M(III) = Co(III), Rh(III), Ir(III), Ru(III). Inorg Chem 1984;23(13):1851–8. http://dx.doi.org/10.1021/ic00181a015.
[48] Minamihata K, Goto M, Kamiya N. Site-specific protein cross-linking by peroxidase-catalyzed activation of a tyrosine-containing peptide tag. Bioconjug Chem 2011;22(1):74–81. http://dx.doi.org/10.1021/bc1003982.
[49] Kersey FR, Loveless DM, Craig SL. A hybrid polymer gel with controlled rates of cross-link rupture and self-repair. J R Soc Interface 2007;4(13):373–80. http://dx.doi.org/10.1098/rsif.2006.0187.